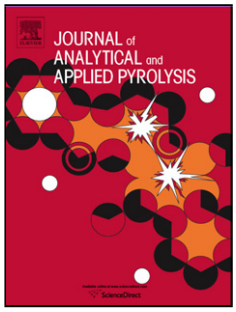

Infrared heated pyrolysis of corn stover: Determination of kinetic and thermodynamic parameters

Erfeng Hu (Conceptualization) (Methodology) (Investigation) (Writing - original draft) (Writing - review and editing), Chongyang Dai (Writing - review and editing), Yishui Tian (Resources) (Funding acquisition) (Supervision), Yang Yang (Formal analysis) (Methodology), Xiaojian Yi (Writing - review and editing), Moshan Li (Writing - review and editing), Si Shao (Writing - review and editing), Yunfei Zhao (Methodology)

PII: S0165-2370(21)00259-X

DOI: https://doi.org/10.1016/j.jaap.2021.105273

Reference: JAAP 105273

To appear in: *Journal of Analytical and Applied Pyrolysis*

Received Date: 21 April 2021

Revised Date: 16 July 2021

Accepted Date: 28 July 2021

Please cite this article as: Hu E, Dai C, Tian Y, Yang Y, Yi X, Li M, Shao S, Zhao Y, Infrared heated pyrolysis of corn stover: Determination of kinetic and thermodynamic parameters, *Journal of Analytical and Applied Pyrolysis* (2021), doi: https://doi.org/10.1016/j.jaap.2021.105273

Infrared heated pyrolysis of corn stover: Determination of kinetic and thermodynamic parameters

Erfeng Hu[1], Chongyang Dai[1], Yishui Tian[2], Yang Yang[3], Xiaojian Yi[1], Moshan Li[1], Si Shao[2], Yunfei Zhao[1]*

1. State Key Laboratory of Coal Mine Disaster Dynamics and Control, Chongqing University, Chongqing 400044, China

2. Academy of Agricultural planning and Engineering, Ministry of Agriculture and Rural Affairs, Beijing 100125, China

3. Bioenergy Research Group, EBRI, Aston University, Birmingham, B4 7ET, UK

**Authors to whom correspondence should be addressed +86-23-6510-2425; email: ehu@cqu.edu.cn (Erfeng Hu)*

Highlights

- Corn stover was performed in an infrared heated pyrolysis system.
- One dimensional diffusion had the greatest degree of fitting among 17 models.
- Bio-oil yield produced by infrared heating reached the maximum value at 550 □.

Abstract: High-value bio-oil and gaseous products can be produced by pyrolysis of corn stover. This work presents a systematic study on pyrolysis characteristics of corn stover using an innovative infrared heated pyrolysis reactor. Firstly, the analytical pyrolysis was performed in a thermogravimetric (TG) analyzer at 10, 20, 30 and 40 °C/min to investigate the thermal

degradation behaviors, and the pyrolysis kinetics and thermodynamics parameters were calculated. The activation energies calculated by FWO and KAS method were 19.61 ~ 38.33 kJ/mol and 11.40 ~ 29.51 kJ/mol respectively at conversion fractions (α) ranging from 0.2 to 0.8, and the one-dimensional diffusion (D1) has the highest fitting degree. The infrared heated technology effectively suppressed the secondary reaction of primary volatiles, and it presented a higher bio-oil yield than electrically heated technology, and as a result, the char and gas yields had a lower value. In both reactors, the yield of bio-oil increases at first and then decreases with the increase in temperature, and the bio-oil yield of the infrared heated furnace and electrically heated furnace reaches the maximum value at 550 □ and 500 □, which are 34.34 wt.% and 26.40 wt.%, respectively. The acids content of bio-oil decreased gradually with the temperature increased in the infrared heated reactor. The yield of phenolic compounds in bio-oil was higher in the former than in the latter, at 19.36% and 14.86%, respectively. The infrared heated reactor has superior performance in producing high quality bio-oils compared to conventional electric heating methods and may be considered as a promising biomass conversion technique.

Keywords: Biomass pyrolysis, kinetic analysis, thermodynamics analysis, product characteristics, infrared heated

Nomenclatures:

M_{ad}: Moisture

A_{ad}: Ash

V_{ad}: Volatile matter

FC: Fixed carbon

ad: Air dried basis

daf: Dry ash-free basis

TG: Thermogravimetric

DTG: Differential thermogravimetry

C-R: Coats-Redfern

FWO: Flynn-Wall-Ozawa

KAS: Kissinger-Akahira-Sunose

α: Conversion degree

g(α): Integral function based on conversion

$f(\alpha)$: Reaction model based on conversion

R^2: Correlation coefficient

β: Heating rate

h: Plank constant

T_p: DTG peak temperature

T_i: Initial decomposition temperature

T_f: Terminal decomposition temperature of the Most intense stage

R_p: Maximum weight loss rate, %/min

$Y_{bio\text{-}oil}$: Yield of bio-oil

Y_{water}: Yield of water

Y_{char}: Yield of char

Y_{gas}: Yield of gas

W_0: Initial sample weight

$W_{bio\text{-}oil}$: Weight of bio-oil

W_{water}: Weight of water

GC: Gas chromatograph

E_a: Apparent activation energy

T: Temperature

R: Universal gas constant

A: pre-exponential factor

ΔH: Changes of enthalpy

ΔG: Changes of Gibbs free energy

ΔS: Changes of entropy

K_B: Boltzman constant

GC-MS: Gas chromatography- mass spectromet

1 Introduction

The significant global consumption of fossil fuels has resulted in the ever-increasing CO_2 emissions and severe air pollutions in many developing countries. Biomass has the advantages of carbon-neutral, renewable, and highly accessible. Processing biomass via pyrolysis technology can produce high-value bio-oil and gaseous products, thus improving the utilization of bio-based resources and reducing the air pollutions caused by open-fired agricultural wastes in many developing countries.

In the last few years, numerous literature has reported the research of biomass pyrolysis and discussed the effect of various processing conditions and materials on the product yields and characteristics.[1-7]. These variables include different heating rate [8], heating temperature [9], pretreatment method [10], and pyrolysis atmosphere [11], all of which have varying effects on the products. The kinetic analysis techniques mainly comprise the model-fitting method and model-free fitting method. The model-fitting method can appropriately match the reaction mechanism model for the material; the great advantage of the model-free fitting method is that there is no risk of choosing the incorrect dynamic model and finding iniquitous dynamic parameters [12-14], and thus the error of kinetic calculation results caused by mechanism function selection can be avoided. FWO technique, KAS method, distributed activation energy method and Friedman method are typical model-free fitting methods [15,16], and much research has shown that FWO and KAS methods are suitable for investigating biomass pyrolysis kinetics [15,17-20]. Ren et al.[21] investigated the thermal decomposition behavior and kinetics of Douglas fir sawdust using TGA and revealed that the

thermal decomposition occurred in two stages with activation energies of 112 kJ/mol and 150 kJ/mol for the first and second reaction stages, respectively. Dhyani et al[22]. studied the thermal decomposition of sorghum straw using non-isothermal thermogravimetric analysis and calculated the kinetic parameters using free-model methods such as Friedman, FWO, KAS. They concluded that the pyrolysis process of sorghum straw can be divided into three zones, each with an average activation energy of 151.21 kJ/mol, 116.15 kJ/mol, and 136.65 kJ/mol. Corn is the second-largest grain around the world, the current treatment techniques for corn stover include direct incineration [23], returning to field[24], fermentation[25]; however, these processes are inefficient in terms of energy. Pyrolysis of corn strove is a promising method of energy conversion. Chen et al.[26] explored the effect of heating rate on the pyrolysis properties of corn stalks with varying moisture contents, and discovered that the thermogravimetric curve shifted toward the high temperature region with increasing temperature. Li et al.[7] investigated the pyrolysis kinetics of corn stover and compared two alternative three-pseudocomponent models, concluding that the three-pseudocomponent model with n-order kinetics was more accurate than the model with first-order kinetics in most cases. Chen et al.[27] researched the pyrolysis characteristics and kinetic parameters of corn stover after acid-washing using Distributed activation energy model method. The findings indicated that acid-washing increased the contents of cellulose and hemicellulose, and decreased the activation energy during pyrolysis. Comprehensive study pyrolysis characteristics and kinetic parameters are required for the development of high-efficiency reactor and process technologies. Thus, it is necessary to fully investigate the pyrolysis kinetics, thermodynamics, and properties of corn stover.

The pyrolysis temperature and solid/vapor residence time in the reactor have significant effects on the volatiles produced and therefore on the yield of pyrolysis liquids and gases. Electrically heated elements are frequently employed to heat the biomass in conventional bench-scale reactors, resulting in a considerable temperature gradient and heat transfer lag, aggravating the secondary reaction of volatiles and decreasing the tar yield. Liu et al. [28] conducted a systematic study of the devolatilization reaction in various reactors and they concluded that the electric heating process presented a large temperature gradient in reactors, resulting in a gas phase temperature that is much higher than the temperature of the processed materials. Secondary reactions occurred and deteriorated when the primary volatiles were exposed to a high-temperature environment and cracked, significantly reducing the yield and composition of the liquid product. Fig.1 illustrates the heating ways in the conventional electrically heated furnace and innovation infrared heated furnace. The heating temperature (T1) and the ambient temperature (T2) and the volatiles release temperature (T3) followed the trend of $T1 > T2 > T3$ in the former; however, the infrared heated furnace showed different ways and followed this trend of $T1 \geq T3 > T2$. This is because the heat transfer way of the infrared furnace is radiation of electromagnetic waves. When the samples absorbed infrared beams and resonated, the particles rapidly reached the setting temperature. In the infrared heated furnace, the pyrolysis volatiles may experience a lower ambient temperature and shorter residence time than that of the electrically heated furnace. Many researchers focused on the infrared heated technology with the goal of minimizing the temperature differential between heat source and materials and thus enabling the direct heating pyrolysis [29,30]. Siramard et al.[31] investigated the oil shale pyrolysis characteristics employing infrared

heating method and discovered that a high heating rate facilitated the generation of volatiles and hydrogen. Xu et al.[32] studied the fast pyrolysis of coal in an infrared heated reactor and established that infrared heating pyrolysis is capable of producing a high tar yield. The infrared heating pyrolysis has attracted much attention from researchers [33]. Zhu et al. [34] investigated the fast pyrolysis behaviors of cedar via rapid infrared heating and found that the higher heating rate of infrared heating is favorable to the production of glucose derivatives. Zhu et al.[35] also studied the infrared heating co-pyrolysis of coal and biomass and discovered that the light tar content in tar was as high as 75.5 wt.%. Infrared heating has the great potential to investigate the precise behavior of biomass pyrolysis. However, limited work has been performed to combine the thermogravimetric analysis, reaction kinetics and thermodynamics, along with pyrolysis behaviors of corn stover via infrared heated pyrolysis experiments, and its conversion mechanism under maximum suppression of secondary reactions of primary volatiles is still unclear and required to further investigation.

The objective of the present study is to combine the thermogravimetric analysis, and reaction kinetics and thermodynamics, along with bench-scale experiments to investigate the pyrolysis characteristics and the effects of heating rate and temperature on corn stover using innovative infrared heated pyrolysis and electrically heated pyrolysis devices. The kinetic parameters were calculated by using the model-fitting method (C-R method) and two model-free methods (FWO and KAS method), and the thermodynamic parameters such as pre-exponential value, Enthalpy change, Gibbs free energy and Entropy change were also evaluated. Moreover, the effects of pyrolysis temperature on corn stover pyrolysis product distribution were researched in the infrared heated pyrolysis reactor and electrically heated

pyrolysis reactor, and its pyrolysis products were analyzed using gas chromatography and gas chromatography-mass spectrometry to study the conversion mechanism.

2. Materials and methods

2.1 Materials

Corn stover utilized in this study was collected from the Daxing District of Beijing, China. The corn stover samples were firstly crushed and screened to below 80 mesh (178 microns), and the proximate analysis and ultimate analyses were carried out on air-dried basis. The results are shown in Table 1. The results of the ultimate analysis showed that carbon, hydrogen and oxygen were the main components in corn stover, among which carbon and oxygen were the most. The corn stover was dried for 12 h at 105 □, prior to the thermogravimetric and pyrolysis experiments.

2.2 Pyrolysis apparatus and procedure

2.2.1 Thermogravimetric analysis

The thermogravimetric experiment was performed on a German Simultaneous (Integrated) Thermal Analyzer STA449F3. Nitrogen (99.999% purity) was used as the carrier gas with a flow rate of 100 mL/min. Approximately 10 mg (±0.1mg) of samples were used in each run. The experiments were conducted from room temperature (25□) to 900 □ at heating rates of 10, 20, 30 and 40 □/min, respectively. The experiments were held at 900 □ for 10 min. Each run was carried out twice, and the error was controlled to be less than 2%.

2.2.2 Pyrolysis experiment

Fig.2 illustrates the schematic diagram of the experimental system. The pyrolysis experiment was performed in a quartz tube reactor (inner diameter 24 mm, length 370 mm), which was heated by an innovative infrared heated furnace (supplied by Shanghai Hanjun Experimental Equipment Co., Ltd). About 3 g (±0.001 g) of the biomass sample was used in each run. High purity nitrogen (99.999 %) was used as the carrier gas with a flow rate of 100 mL/min. After removing the air from the reactor, it was heated to the pyrolysis temperature (400~600 °C) at a heating rate of 30 °C/min, and it holds for 20 minutes to ensure the biomass samples fully convert. The pyrolysis vapor condensed was collected in a U-shaped tube submerged in ethylene glycol at a temperature of -25 °C. The non-condensable gas passed through three acetone washing beakers before being measured using a wet gas flowmeter. A Micro-GC was adopted to determine the gas composition. The parallel pyrolysis experiment was also conducted in a conventional electrically heated furnace under identical processing conditions for comparison.

2.3 Kinetic analysis method

The kinetic of corn stover pyrolysis was determined by Arrhenius law, which provided information about the rate of reaction. Based on the basic equation used for kinetic analysis of steam analysis, the results were obtained:

$$\frac{d\alpha}{dt} = A\exp\left(-\frac{E_a}{RT}\right) f(\alpha) \qquad (1)$$

where A is the pre-exponential factor (min^{-1}), α is the conversion rate at time t, E_a is apparent activation energy (kJ/mol), R is the universal gas constant (0.008314 kJ/mol*K) and T is

reaction temperature (K).

Integrating Eq. (1), the integral function g(α) can be defined as follows:

$$g(\alpha)=\int_0^{\alpha}\frac{d\alpha}{f(\alpha)}=A\int_0^{t}\exp\left(-\frac{E_a}{RT}\right)dt \quad (2)$$

For constant heating rate:

$$\beta=\frac{dT}{dt} \quad (3)$$

Integrative equations (1) and (3)

$$\frac{d\alpha}{dT}=\frac{A}{\beta}\exp\left(-\frac{E_a}{RT}\right)f(\alpha) \quad (4)$$

$$g(\alpha)=\int_0^{\alpha}\frac{d\alpha}{f(\alpha)}=\frac{A}{\beta}\int_0^{T}\exp\left(-\frac{E_a}{RT}\right)dT \quad (5)$$

where β is the heating rate, $g(\alpha)$ is α kinetic function of different reaction mechanisms which is obtained from integration of f(α).

2.3.1 Model-fitting model: Coats-Redfern method

The basic equation for the Coats and Redfern method is[36]:

$$\ln\left[\frac{g(\alpha)}{T^2}\right]=\ln\frac{AR}{\beta E_a}\left(1-\frac{2RT}{E_a}\right)-\frac{E_a}{RT} \quad (6)$$

E_a can be obtained by plotting 1/T versus $\ln[g(\alpha)/T^2]$. Most of the solid-state degradation reactions are listed in Table 2.

2.3.2 Flynn-Wall-Ozawa (FWO) method

Integrate equation (5) and substitute it into Doyle's [37,38]approximation:

$$\lg\beta=\lg\left[\frac{AE_a}{g(\alpha)R}\right]-2.315-0.4567\frac{E_a}{RT} \quad (7)$$

E_a can be calculated from the slope by plotting $\lg\beta$ versus $1/T$.

2.3.3 Kissinger-Akahira-Sunose (KAS) method

$$\ln\left(\frac{\beta}{T^2}\right)=\ln\left(\frac{AR}{E_a g(\alpha)}\right)-\frac{E_a}{RT} \quad (8)$$

Plotting $\ln\left(\frac{\beta}{T^2}\right)$ versus $1/T$, E_a can be obtained from the slope [39]. The relevant parameters with the α of 0.2~0.8 were selected to conduct kinetic calculation."

2.4 Thermodynamics analysis

The thermodynamic parameters including the pre-exponential factor (A), change of enthalpy (ΔH), Gibbs free energy(ΔG) and entropy (ΔS). They are calculated as follows[40]:

$$A=\beta E_a \exp\left(\frac{E_a}{RT_P}\right)/\left(RT_P^2\right) \quad (9)$$

$$\Delta H=E_a-RT \quad (10)$$

$$\Delta G=E_a+RT_P\ln\left(\frac{K_B T_P}{hA}\right) \quad (11)$$

$$\Delta S=\frac{\Delta H-\Delta G}{T_P} \quad (12)$$

where K_B is the Boltzman constant (1.281×10^{-23} J/K), h is Plank constant (6.626×10^{-34} J/s), T_p is the DTG peak temperature, and T is the temperature at the conversion degree.

2.5 Product analysis and characterization

The liquid products (water and bio-oil) were determined by the weight difference before and after the U-shape tube, and the weight of char was obtained by weighing the remaining solid products after the pyrolysis experiment completed. The weight of the bio-oil was

calculated as the difference between the overall weight of the liquid product and the weight of the water contained therein. The water content in the liquid product was determined by Karl-Fischer micro-moisture tester (KSL 701, Zibo Kulun). Prior to the analysis, the electrolyte was calibrated with purified water until the electrolytic equilibrium was achieved. The injection volume was 20 μL, and the same sample was analyzed for five times. The average value was calculated for three data points with a discrepancy of less than 0.1 percent. The average value is the water content of the liquid.

$$C_{water} \times W_{liquid} = W_{water} \quad (13)$$

Where C_{water} is the water content of the liquid determined by Karl-Fischer micro-moisture machine, W_{liquid} is the weight of liquid products (water and bio-oil), W_{water} is the weight of water in liquid products. The distribution of pyrolysis products is calculated on a dry ash-free basis with the method followed in a previous study [34]. The weight of the bio-oil may be estimated as the difference between the overall weight of the liquid product and the weight of the water contained therein. The composition of the bio-oil was determined by gas chromatography-mass spectrometry (GC-MS Shimadzu, GCMS-QP2010 Plus). The GC oven temperature started from 50 □ and held for 5 minutes, then heated to 260 □ at 5 □/min. The terminal temperature was maintained for 5 minutes. The injection volume of the sample was 1 μL. High-purity helium was used as carrier gas with a flow rate of 1 mL/min. The split mode and the split ratio was 10:1. The inlet temperature was 230 □. Rtx-WAX (30 mm × 0.25 mm × 0.25 μm) was utilized as the chromatographic column. Mass spectrometric collection range m/z: 35-500. The NIST mass spectral library was used to compare the spectral data in order to identify the bio-oil compounds. The area normalization method (relative peak area, %) was

employed to estimate the relative yields of different compounds. Gas compositions were analyzed by a Micro-GC (Inficon 3000).

3 Results and discussion

3.1 Pyrolysis characteristics of corn stover

Fig.3 illustrates the TG and DTG curves for pyrolysis of corn stover at various heating rates. As observed, the whole pyrolysis process of corn stover may be divided into three stages and the main pyrolysis reactions occurred between 240 □ and 400 □. The first stage is water removal, during which the corn stover structure is dehydrated and gently torrefied to loosen it. The second stage of corn stover pyrolysis reaction was violent [41], and the main reactions were the decomposition of hemicellulose and cellulose, accompanied by the extremely slow decomposition of a portion of lignin. Volatiles were released in significant quantities as condensable liquid and gas, accounting for 50% of the sample mass. The third stage (>400 □) was characterized by the decomposition, aromatization, and carbonization reaction of lignin, as well as the generation of coke and permanent gases. This is confirmed by the findings of Hu et al.[42], who showed that lignin decomposes more slowly than hemicellulose and cellulose between 160 and 900 °C. As shown in Fig. 3b, the predominant weight loss stages get wider with the increase of temperature. This is due to the thermal hysteresis effect (heat transfer restriction) produced by high heating rates, which may cause the pyrolysis temperature range to shift to the right hand side of the figure [43,44]. It is worth noting that inflection points in the DTG curve of each heating rate are observed at about 285 ~ 320 □, indicating that a significant quantity of cellulose started decomposing quickly after

this temperature. After hemicellulose and cellulose decomposed entirely at about 380 °C, lignin decomposition dominated the TG curve.

Table 3 lists the key characteristic parameters of the DTG curves at different heating rates. The initial temperature of decomposition rose progressively from 269.40 □ to 287.30 □ as the heating rate increased from 10 □/min to 40 □/min. The temperature of terminal decomposition of corn stover at various heating rates likewise followed the same trend. A greater heating rate resulted in a shift of the TG and DTG curves to the right, demonstrating that a higher temperature is required to start the devolatilization of samples at a higher heating rate. Additionally, it was also shown that increasing the heating rate led to thermal hysteresis, which elevated the initial decomposition temperature when the heating rate was increased[45].On the other hand, this phenomenon may be explained by the fact that the feedstock cannot fully react in a short time as the heating rate rises, creating the appearance of an increase in the initial decomposition temperature. At 10, 20, 30 and 40 □/min, the maximum weight loss rates were 330.36 □, 340.20 □, 353.25 □ and 358.07 □, respectively, and the corresponding maximum weight loss rates were -6.50, -15.51, -21.75, and -31.29 wt.%/min. As the heating rate rises, the temperature at which the corn stover reaches the maximum weight loss rate also increases, this finding is consistent with previous research [46-48]. The maximal rate of weight loss increased considerably, this is because the increased heating rate intensified the pyrolysis reaction[49].

3.2 Kinetic and thermodynamics analysis

3.2.1 Coats-Redfern method

The kinetic characteristics of corn stover pyrolysis at various heating rates were calculated using seventeen distinct reaction models. To ensure that the results accurately reflect the pyrolysis process, only the data from the primary weight loss phases (in the TG curve) were utilized for kinetic computation, this is because the pyrolysis reaction occurs mainly at this stage and is unaffected by weight loss due to dehydration and degassing processes. As shown in Table 4, the calculated results include the apparent activation energy E_a and the correlation coefficient R^2. The correlation coefficients of reaction models A3/2, F2, F3 are relatively low in comparison to the other reaction models, which all have correlation coefficients near to or more than 0.9 regardless of the change in heating rate. It was worth noting that the correlation coefficients for different heating rates for the same model were extremely similar, indicating that the heating rate had little effect on the reaction process. Notably, the reaction model of one-dimensional diffusion (D1) has the highest correlation coefficients of 0.994, 0.988, 0.991 and 0.984, corresponding to the temperature of 10, 20, 30 and 40 □/min respectively, and the E_a value range from 13.28 ~ 15.76 kJ/mol, it demonstrates that the one-dimensional diffusion model accurately describes the primary devolatilization stage of corn stover pyrolysis.

3.2.2 Flynn-Wall-Ozawa and Kissinger-Akahira-Sunose method

Fig. 4 shows the fitted FWO and KAS models for the pyrolysis of corn stover. Cai et al.[50] found that while calculating kinetics, it was necessary to remove the moisture

evaporation zone, and Abd-Elghany et al.[51] recommended utilizing data with a conversion rate of 0.3~0.7. To avoid being affected by the dehydration and carbonization stages, the data for conversion rate 0.2~0.8 is selected in this study for kinetics analysis. Table 5 shows the activation energy, average activation energy, and fitting correlation coefficients versus the 0.2~0.8 conversion rate using the FWO and KAS methods. Correlation coefficients for each conversion rate were found to be more than 0.95, indicating that the calculated results were highly reliable. The activation energies calculated by FWO and KAS were 18.10~8.33 kJ/mol and 11.40~29.51 kJ/mol, with average activation energies of 25.57 kJ/mol and 17.15 kJ/mol, respectively. When the conversion rate was 0.2, the activation energy was the lowest, indicating that the pyrolysis process occurred more easily at this time.

The activation energy values were greatest for both methods when the conversion rate was 0.8, suggesting that more energy is required for the pyrolysis process at this time. Fig 5 illustrates the change in activation energy with the conversion rate. In general, the activation energy value fluctuates with the increase in the conversion rate, this is because the three main components of biomass (hemicellulose, cellulose, and lignin) have distinct pyrolysis characteristics [52], also indicating that the pyrolysis process is extremely complicated in terms of kinetics [53]. In addition, the activation energy curves produced using the two techniques had an identical trend. Islam et al.[54] investigated pericarp pyrolysis using TGA and analyzed the results using FWO and KAS methods. The results indicated that the activation energy of the pericarp was 61.06 kJ/mol for KAS method and 135.87 kJ/mol and FWO method, respectively, and these values are much higher than those obtained from corn stover pyrolysis.

3.2.3 Thermodynamics parameters

As discussed in section 3.1, thermal processing at a high heating rate may cause thermal hysteresis[55]. As a result, the TGA data at the lowest heating rate (10 □/min) were selected to calculate the thermodynamic parameters, as shown in Table 6. Fig.6 illustrates the changes in the thermodynamic parameters of corn stover pyrolysis using FWO and KAS methods.

3.2.3.1. Pre-exponential value

The change of Arrhenius pre-exponential factor (expressed as log10) with the conversion rate is shown in Fig. 6a. For FWO and KAS methods, the pre-exponential values varied from 92544.99 s^{-1} to 180922.76 s^{-1} and 53813.44 s^{-1} to 139266.40 s^{-1} respectively. Due to the complicated chemical composition of corn stover, a wide range of pre-exponential values has been found. As the pyrolysis reaction processes, hemicellulose and cellulose decompose first, requiring a great deal of energy. When the conversion factor approaches 0.4, the amount of energy needed decreases. After reaching 0.6, the pre-exponential factor started to rise again, which was ascribed to the decomposition of residual lignin. This trend demonstrated that various level of energy was required for different stages of corn stover pyrolysis.

3.2.3.2 Enthalpy change

Fig. 6b shows the change of enthalpy with the conversion rate. Enthalpy value represents the quantity of the heat absorbed or released at constant pressure[56]. The values enthalpy change (ΔH) calculated using FWO method and KAS method were 15.05~32.97 kJ/mol and 6.84~24.14 kJ/mol, respectively. A positive ΔH suggests that energy from an external source is required to convert the reagents from their higher energy state to their transition state. The

enthalpy changes calculated using the two methods were all positive, showing that the pyrolysis reaction of corn stover was endothermic, with the molecules absorbing heat and breaking down to create new chemical bonds. The difference between activation energy and enthalpy for the two methods is negligible in this study. The maximum differences between enthalpy and activation energy at various conversion rates are 5.56 kJ/mol and 5.37 kJ/mol for the FWO and KAS methods, respectively, which agrees well with the findings reported by Mehmood et al[57].

3.2.3.3. Gibbs free energy

The Gibbs free energy (ΔG) reveals the total increase in energy caused by the reagents approaching and forming the activated complex[58]. The ΔG values obtained by FWO method ranged from 113.09 ~ 128.46 kJ/mol, with an average value of 117.99 kJ/mol. The values obtained using KAS method were 107.60 ~ 120.94 kJ/mol, with an average of 111.51 kJ/mol. Fig. 6c shows the change of ΔG with the conversion. It is worth noting that the change tendencies determined by the two methods were identical, and the difference between the maximum and minimum values of ΔG was insignificant. All of these results indicated that the energy output throughout the whole reaction process was relatively stable [59], showing that corn stover had great potential for biomass energy. As a result, further pyrolysis experiments and product analyses of corn stover are required.

3.2.3.4. Entropy change

Entropy change (ΔS) may be used to measure the degree of disorder in a system. As shown in Fig. 6d, the trend of entropy change with conversion rate has been displayed. The

ΔS of FWO method is -162.63 ~ -158.40 J/K, and the KAS method has a value of -167.14 ~ -160.57 J/K. The values of ΔS shown in Table 6 are all negative, it is confirmed that the dissociated product has a lower disorder degree than the initial reactant[60]. Meanwhile, these negative values imply that the disintegration in the activated state has a more well-organized structure than it had prior to the thermal disintegration.

3.3 Pyrolysis products analysis

3.3.1 Effect of temperature on products distribution

The thermodynamic analysis indicates that the corn stover has stable energy output, and despite the fact that mg-level amount of sample was fed in TG experiment, the thermal lag was observed in DTG curve, and it was postulated that the thermal hysteresis had a negative effect on the pyrolysis products. As a result, verification in a bench-scale reactor with g-level is critical, and the reactors with direct heating (infrared heating) and indirect heating (electric heating) were adopted to investigate the pyrolysis behavior of corn stover.

Fig.7 illustrates the product distribution (water, bio-oil, char and gas) from pyrolysis of corn stover at various terminal temperatures using infrared and electrically heated furnaces. The bio-oil yield of the two furnaces showed a similar changing trend, increasing first and then decreasing with temperature increasing. The bio-oil yield of infrared heated furnace rose gradually from 400 □ to 550 □, reaching a maximum value of 34.34 wt.% at 550 □, while the highest bio-oil yield of electrically heated furnace is only 26.40 wt.% at 500 □. The secondary gas-phase reactions of the primary product in corn strove pyrolysis become intensified when the pyrolysis temperature exceeds 500 □, promoting tar cracking and gas

generation. As the temperature increased from 400 □ to 600 □, the gas yield rose from 14.86 wt.% to 23.68 wt.% and 21.54 wt.% to 30.38 wt.% for infrared heated furnace and electrically heated furnace respectively, but the yield of char is opposite to the variation of gas. With increasing temperature from 400 □ to 600 □, the yield of water decreases gradually from 25.60 wt.% to 22.07 wt.% for infrared heated furnace, the similar behavior was also observed when Zhu et al. [34,35] explored the infrared heating pyrolysis of biomass. As the temperature rises, the yield of water in the electrically heated furnace varies between 20.40 wt.% and 22.90 wt.%. Increased pyrolysis temperature offers more extra energy for breaking the stronger bonds in macromolecular substances, which improves the formation of small molecules gases. Additionally, with increasing temperature, water vapor may react weakly with carbon, generating a small amount of non-condensable gas [34]. Significantly, the bio-oil yield produced by an electrically heated furnace is lower than that produced by an infrared heated furnace at all temperatures, while the char and gas yields produced by the electrically heated furnace are higher than those produced by an infrared heated furnace. The phenomenon of thermal hysteresis occurred as a result of the indirect heating condition through electric heating, making the volatiles experience a higher ambient temperature after it escaped from particles inside, aggravating the secondary reaction of primary pyrolysis products. In comparison, the infrared beam radiates directly on the material, causing its molecules to resonate and direct heating in a short time. When volatiles escaped from material particles, the ambient temperature experienced by it is lower than the interior, thus reducing the secondary reaction of primary volatiles [28,34,35]. As a consequence, an infrared heated furnace produces more bio-oil than an electrically heated furnace, but an electrically heated

furnace produces more char and gas.

3.3.2 Bio-oil analysis

The main components of bio-oil are grouped as phenols, acids, ketones, aldehydes, alcohols, and their relative contents are shown in Fig. 8. The total ion chromatograms (TICs) of bio-oil were shown in Fig. S1 and Fig. S2. Ketones and acids made up the majority of these components, followed by phenols and alcohols. As can be observed, oxygen-containing compounds in bio-oil account for a remarkable proportion, this is because cellulose includes a high amount of oxygen-containing structural units such as glucose, cellobiose in hemicellulose and guaiacol in lignin[61]. Due to the high acid content, the bio-oil is tough to utilize directly as a transportation fuel. The content of acids in infrared heated furnace decreases noticeably with the increase in temperature, this is attributed to the fact that the small molecular acids are primarily derived from the pyrolysis of cellulose and hemicellulose in corn stover. After 400 □, the products from pyrolysis of cellulose and hemicellulose gradually decrease, while those from lignin pyrolysis take a dominant position, which is also shown in the result of TG. In comparison, the content of acids in an electrically heated furnace decreases slightly with varying temperatures. Although the ketone content of an electrically heated furnace decreases as the temperature rises, it is still more than that of an infrared heated furnace. Wang et al.[62] found that the three major components of lignin are phydroxyphenylpropane, guaiacylpropane and syringylpropane,thus, the decomposition of lignin may produce more phenols than the decomposition of cellulose and hemicellulose. There is a slight reduction in phenols at 600 □ in an infrared heated furnace, suggesting that the majority of the lignin has been pyrolyzed prior to 600 □. The phenols in the electrically

heated furnace vary within a small range as the temperature changes. The bio-oil produced by an infrared heated method contains more phenols than that produced by an electrically heated furnace at 500~600 □, this could be due to the reason that infrared heating can better promote the decomposition of the lignin structure and resulting higher amount of phenolic compounds in the bio-oil. The higher phenols content enables the utilization of bio-oil, as phenolic compounds can be used as raw materials for the production of many high-value chemical and industrial products such as fragrances, essential oils, stabilizers, antioxidants, anesthetics, as reported in the relevant literature [63].

3.3.3 Gas analysis

Fig.9 shows variations of gas composition with varying temperatures. The pyrolysis gases include carbon dioxide, carbon monoxide, methane and C_2-C_3 (C_2H_4, C_2H_6, C_3H_6 and C_3H_8). It can be seen that CO_2 accounts for a significant part of the gaseous products. CO_2 was generated primarily via the cleavage of carbonyl and carboxyl groups in the main chain and side chain macromolecules, as well as the rapture of C-O bond in cellulose and hemicellulose [64]. The CO_2 yield of the infrared heated furnace decreases gradually with the increase in temperature. The electrically heated furnace produces considerably more CO_2 than the infrared heated furnace at 600 □, which may be attributed to the excessively long reaction time of volatiles at high temperatures. There was no discernible variation in CO, H_2, CH_4 and C_2-C_3 contents between the two furnaces. The maximum yield of CO produced in an infrared heated furnace is 34.10 vol.% at 550 □, and the highest yield of CH_4 and H_2 is 10.04 vol.% and 10.46 vol.% at 600 □ respectively, the maximum yield of CO, H_2, CH_4 produced in an electrically heated furnace is 28.97 vol.%, 11.18 vol.%, 10.24 vol.%, respectively. CH_4 is

mainly generated through alkyl chain conversion, the removal of methoxy (CH_3O-) substituents, and the degradation of methyl (-CH_3), methylene (-CH_2-) in lignin [17,65]. Due to the decomposition of lignin at high temperatures, the yield of CH_4 is higher in the high temperature region. The yield of C_2-C_3 remains relatively constant with temperature increase, and the electrically heated furnace presents a slightly higher content than that of the infrared heated furnace.

4 Conclusion

The effects of heating rate and temperature on corn stover pyrolysis were studied using TG and an innovative infrared heated pyrolysis reactor, in comparison to a conventional electrically heated pyrolysis reactor. The one-dimensional diffusion (D1) had the greatest degree of fitting among the 17 reaction mechanism models. The values of activation energy were calculated using FWO and KAS methods and were 19.61 ~ 38.33 kJ/mol and 11.40 ~ 29.51 kJ/mol, respectively, and the ΔH values ranged from 15.05 to 32.97 kJ/mol and 6.84 to 24.14 kJ/mol, and the ΔG values ranged from 113.09 to 128.46 kJ/mol and 107.60 to 120.94 kJ/mol for FWO and KAS methods, respectively, indicating that corn stover had great potential for biomass energy application. The results of pyrolysis experiments showed that infrared heating suppressed the secondary reaction of primary volatiles and that infrared heating generated more bio-oil than electrical heating, whereas electrical heating produced more gas and char. The infrared heated furnace produced the highest yields of bio-oil at 34.34 wt.% and the electrically heated furnace produced the greatest yields at 26.49 wt.%, respectively. The CO_2 content of the infrared heated furnace decreased gradually with the increase in temperature, reaching a minimum of 65.10 vol.% at 600 □, while the yields of H_2

and CH_4 increased to 10.46 vol.% and 10.04 vol.%, respectively. Bio-oil produced in the infrared heated furnace has similar components with electrically heated furnace and is mostly grouped as ketones, phenols, acids, alcohols, aldehydes, etc. Both heating methods have the highest yield of acids at 400 □, at 36.40% and 30.28%, respectively. The maximum content of phenols in bio-oil of the two furnaces was 14.86% via electrically heating and 19.36% via infrared heating, respectively, suggesting that the infrared heated reactor has superior performance on producing high-quality bio-oils compared to using conventional electrical heating means and may be regarded a promising biomass conversion technique. Given the benefits of generating high-yield bio-oil in an infrared heating reactor, it is worthwhile to do further research to investigate catalytic pyrolysis and bio-oil quality improvement using this technology.

CRediT author statement

Erfeng Hu: Conceptualization, Methodology, investigation, Writing- original draft, Writing- review & editing. Chongyang Dai: Writing- review & editing. Yishui Tian: Resources, Funding acquisition, Supervision. Yang Yang: Formal analysis, Methodology. Xiaojian Yi: Writing- review & editing. Moshan Li: Writing- review & editing. Si Shao: Writing- review & editing. Yunfei Zhao: Methodology.

Declaration of interests

The authors declare that they have no known competing financial interests or personal relationships that could have appeared to influence the work reported in this paper.

Acknowledgement

The authors gratefully acknowledge the financial support provide by the National Modern Agricultural Industrial Technology System (CARS-03-40)，National Natural Science Foundation of China (Nos. U19B2009) and the Fundamental Research Funds of Chongqing City (Nos. CX2019125 and 2019LY41).

References

[1] T. Kan, V. Strezov and T.J. Evans, *Renewable & Sustainable Energy Reviews*, 57, (2016) 1126.

[2] Y. Zhang, P. Chen, S. Liu, L. Fan, N. Zhou, Y. Cheng, P. Peng, E. Anderson, Y. Wang and Y. Liu, *Microwave-Assisted Pyrolysis of Biomass for Bio-Oil Production*, 2017, p.

[3] S. Stegen and P. Kaparaju, *Fuel*, 276, (2020) 118112.

[4] T. Yuan, A. Tahmasebi and J. Yu, *Bioresour Technol*, 175, (2015) 333.

[5] A. Garcia-Maraver, J.A. Perez-Jimenez, F. Serrano-Bernardo and M. Zamorano, *Renewable Energy*, 83, (2015) 897.

[6] K. Slopiecka, P. Bartocci and F. Fantozzi, *Applied Energy*, 97, (2012) 491.

[7] Z. Li, W. Zhao, B. Meng, C. Liu, Q. Zhu and G. Zhao, *Bioresource Technology*, 99,

(2008) 7616.

[8] D. Chen, J. Zhou and Q. Zhang, *Bioresource Technology*, 169, (2014) 313.

[9] Z. Ma, D. Chen, J. Gu, B. Bao and Q. Zhang, *Energy Conversion & Management*, (2015).

[10] A. Zheng, K. Zhao, L. Li, Z. Zhao, L. Jiang, Z. Huang, G. Wei, F. He and H. Li, *Journal of the Energy Institute*, (2018).

[11] C. Guizani, F.J. Escudero Sanz and S. Salvador, *Fuel*, 116, (2014) 310.

[12] H. Liu, G. Xu and G. Li, *Process Safety and Environmental Protection*, 149, (2021) 48.

[13] J. Nisar, A. Rahman, G. Ali, A. Shah, Z.H. Farooqi, I.A. Bhatti, M. Iqbal and N. Ur Rehman, *Biomass Conversion and Biorefinery*, (2020).

[14] J. Nisar, F. Ali, M.A. Malana, G. Ali, M. Iqbal, A. Shah, I.A. Bhatti, T.A. Khan and U. Rashid, *Biomass Conversion and Biorefinery*, 10, (2020) 1179.

[15] Q. He, L. Ding, Y. Gong, W. Li, J. Wei and G. Yu, *Bioresource Technology*, 280, (2019) 104.

[16] S. Lv, Y. Zhang and H. Tan, *Waste Management*, 87, (2019) 335.

[17] Z. Ma, D. Chen, J. Gu, B. Bao and Q. Zhang, *Energy Conversion and Management*, 89, (2015) 251.

[18] R.K. Mishra and K. Mohanty, *Bioresource Technology*, 251, (2018) 63.

[19] G. Ali, J. Nisar, A. Shah, M. Abbas, M. Raza, U. Rashid, I. Ahmad, R. Khan and F. Shah, *Waste Management & Research*, 38, (2019) 0734242X1986533.

[20] J. Nisar, G. Ali, A. Shah, M.R. Shah, M. Iqbal, M.N. Ashiq and H.N. Bhatti, *Energy &*

Fuels, 33, (2019) 12666.

[21] S. Ren, H. Lei, L. Wang, Q. Bu, S. Chen and J. Wu, *Biosystems Engineering*, 116, (2013) 420.

[22] V. Dhyani, J. Kumar and T. Bhaskar, *Bioresource Technology*, (2017) 1122.

[23] X.D. Cui and Y.Y. Teng, *Academic Periodical of Farm Products Processing*, (2013).

[24] S. Wang, X. Huang, Y. Zhang, C. Yin and A. Richel, *Resources, Conservation and Recycling*, 167, (2021) 105402.

[25] H. Guo, S. Zhao, Z. Dong, Q. Wang, D. Xia, J. Jia, X. Yin and H. Yu, *Renewable Energy*, 161, (2020) 701.

[26] D. Chen, T. Long and X. Zhu, *Energy Sources*, 37, (2015) 1332.

[27] D. Chen, D. Gao, S. Huang, S.C. Capareda, X. Liu, Y. Wang, T. Zhang, Y. Liu and W. Niu, *Journal of Analytical and Applied Pyrolysis*, 155, (2021) 105027.

[28] Z. Liu, X. Guo, L. Shi, W. He, J. Wu, Q. Liu and J. Liu, *Fuel*, 154, (2015) 361.

[29] J.L. Zhu, L.J. Jin, Y.W. Luo, H.Q. Hu, Y.K. Xiong, B.Y. Wei and D.C. Wang, *Energy Conversion and Management*, 205, (2020).

[30] J.G. Li, J.L. Zhu, H.Q. Hu, L.J. Jin, D.C. Wang and G.J. Wang, *Fuel*, 272, (2020).

[31] S. Siramard, Y. Bunman, D. Lai and G. Xu, *Energy & Fuels*, 31, (2017) 6996.

[32] S. Xu, X. Zeng, Z. Han, J. Cheng, R. Wu, Z. Chen, O. Masek, X. Fang and G. Xu, *Applied Energy*, 242, (2019) 732.

[33] J. Li, J. Zhu, H. Hu, L. Jin, D. Wang and G. Wang, *Fuel*, 272, (2020) 117739.

[34] J. Zhu, L. Jin, J. Li, Z. Bao and H. Hu, *Bioresource Technology*, 290, (2019) 121739.

[35] J. Zhu, L. Jin, Y. Luo, H. Hu, Y. Xiong, B. Wei and D. Wang, *Energy Conversion and*

Management, 205.

[36] A.W. Coats and J.P. Redfern, *Nature*.

[37] C.D. Doyle, *Journal of Applied Polymer Science*, 6, (1962) 639.

[38] W. Miao, X. Li, Y. Wang and Y. Lv, *Journal of Petroleum Science and Engineering*, 182, (2019) 106309.

[39] Kissinger and E. H., *Analytical Chemistry*, 29, (1957) 1702.

[40] Y.S. Kim, Y.S. Kim and S.H. Kim, *Environ Sci Technol*, 44, (2010) 5313.

[41] N. Sophonrat, L. Sandstrom, I.N. Zaini and W.H. Yang, *Applied Energy*, 229, (2018) 314.

[42] M. Hu, Z. a, S. b, D. Guo, C. a, Y. a, J. a, M. Laghari, S. Fazal, B. a, B. a and S. Ma, *Energy Conversion and Management*, 118, (2016) 1.

[43] C.T. Chong, G.R. Mong, J.H. Ng, W.W.F. Chong, F.N. Ani, S.S. Lam and H.C. Ong, *Energy Conversion & Management*, 180, (2019) 1260.

[44] H. Shahbeig and M. Nosrati, *Renewable and Sustainable Energy Reviews*, 119, (2020) 109567.

[45] X. Huang, J.P. Cao, X.Y. Zhao, J.X. Wang, X. Fan, Y.P. Zhao and X.Y. Wei, *Fuel*, 169, (2016) 93.

[46] X. Hanmin, M. Xiaoqian and L. Kai, *Energy Conversion & Management*, 51, (2010) 1976.

[47] Z.Q. Ma, J.H. Wang, Y.Y. Yang, Y. Zhang, C. Zhao, Y.M. Yu and S.R. Wang, *Journal of Analytical and Applied Pyrolysis*, 134, (2018) 12.

[48] G. Chen, S. He, Z. Cheng, Y. Guan, B. Yan, W. Ma and D.Y.C. Leung, *Bioresour*

Technol, 243, (2017) 69.

[49] C.T. Chong, G.R. Mong, J.-H. Ng, W.W.F. Chong, F.N. Ani, S.S. Lam and H.C. Ong, *Energy Conversion and Management*, 180, (2019) 1260.

[50] J.M. Cai, D. Xu, Z.J. Dong, X. Yu, Y. Yang, S.W. Banks and A.V. Bridgwater, *Renewable & Sustainable Energy Reviews*, 82, (2018) 2705.

[51] M. Abd-Elghany, T.M. Klaptke and A. Elbeih, *Propellants Explosives Pyrotechnics*, (2017).

[52] D.K. Shen, S. Gu, B. Jin and M.X. Fang, *Bioresource Technology*, 102, (2011) 2047.

[53] S. Papari and K. Hawboldt, *Renewable and Sustainable Energy Reviews*, 52, (2015) 1580.

[54] M.A. Islam, M. Asif and B.H. Hameed, *Bioresour Technol*, 179, (2015) 227.

[55] H.L. Cao, Y. Xin, D.L. Wang and Q.X. Yuan, *Bioresource Technology*, 172, (2014) 219.

[56] Hui, Li, Sheng-li, Niu, Chun-mei, Lu, Shi-qing and Cheng, *Energy Conversion & Management*, (2015).

[57] M.A. Mehmood, M.S. Ahmad, Q. Liu, C.G. Liu and M. Gull, *Energy Conversion and Management*, 194, (2019) 37.

[58] S.C. Turmanova, S.D. Genieva, A.S. Dimitrova and L.T. Vlaev, *eXPRESS Polymer Letters*, 2, (2008) 133.

[59] Kaur, Ravneet, Gera, Poonam, Jha, Mithilesh, Kumar, Bhaskar and Thallada, *Bioresource Technology Biomass Bioenergy Biowastes Conversion Technologies Biotransformations Production Technologies*, (2018).

[60] A.A.D. Maia and L.C. De Morais, *Bioresource Technology*, 204, (2016) 157.

[61] S. Wang, G. Dai, H. Yang and Z. Luo, *Progress in Energy and Combustion Science*, 62, (2017) 33.

[62] S. Wang, B. Ru, G. Dai, Z. Shi, J. Zhou, Z. Luo, M. Ni and K. Cen, *Proceedings of the Combustion Institute*, (2016) 2225.

[63] F. Ate, N. Miskolczi and B. Saricaolu, *Bioresource Technology*, 177, (2015) 149.

[64] P. Fu, W. Yi, X. Bai, Z. Li, S. Hu and J. Xiang, *Bioresource Technology*, 102, (2011) 8211.

[65] F. Song, T. Li, J. Zhang, X. Wang and F. Wu, *Environmental Science and Technology*, 2019, (2019).

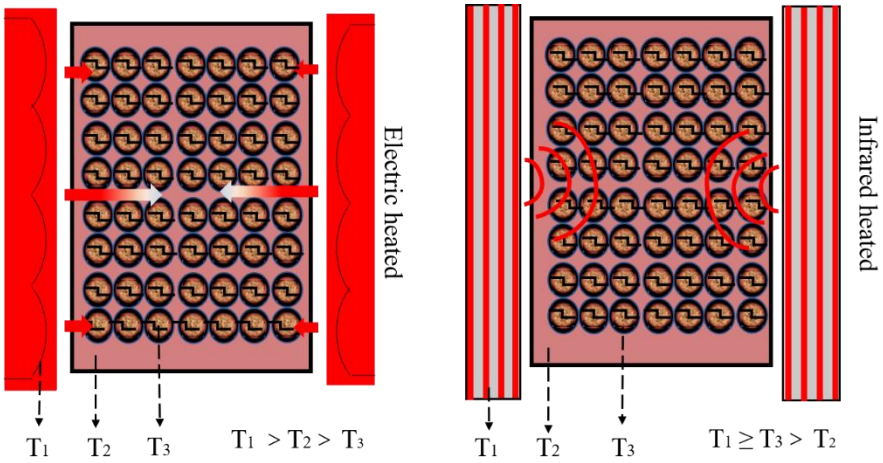

Figure 1. Heating ways in conventional electrically heated furnace and innovation infrared heated furnace T_1: heating temperature, T_2: ambient temperature, T_3: volatiles releasing temperature

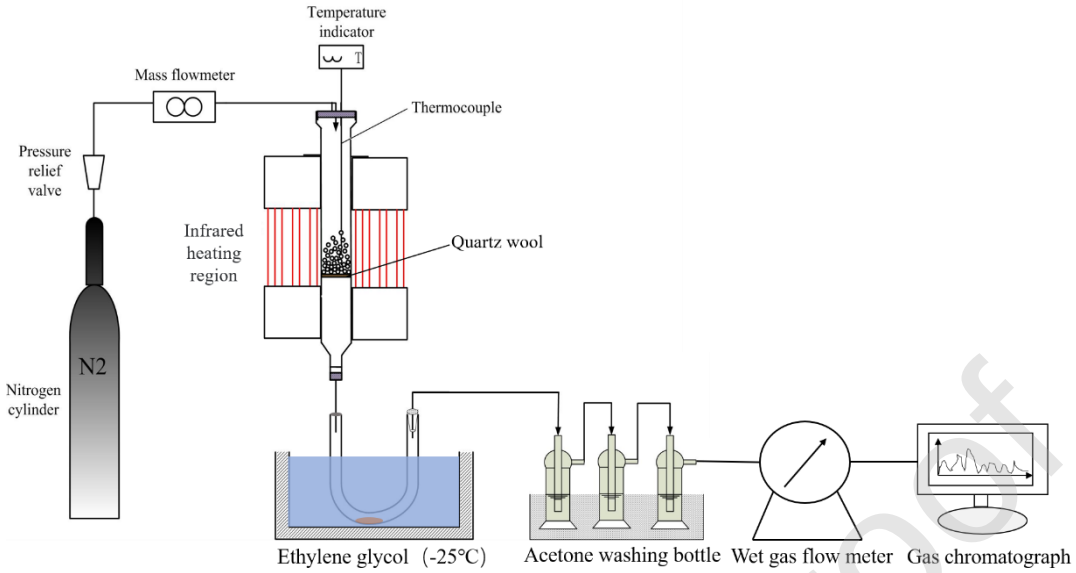

Figure 2 Schematic diagram of the infrared heated pyrolysis rig

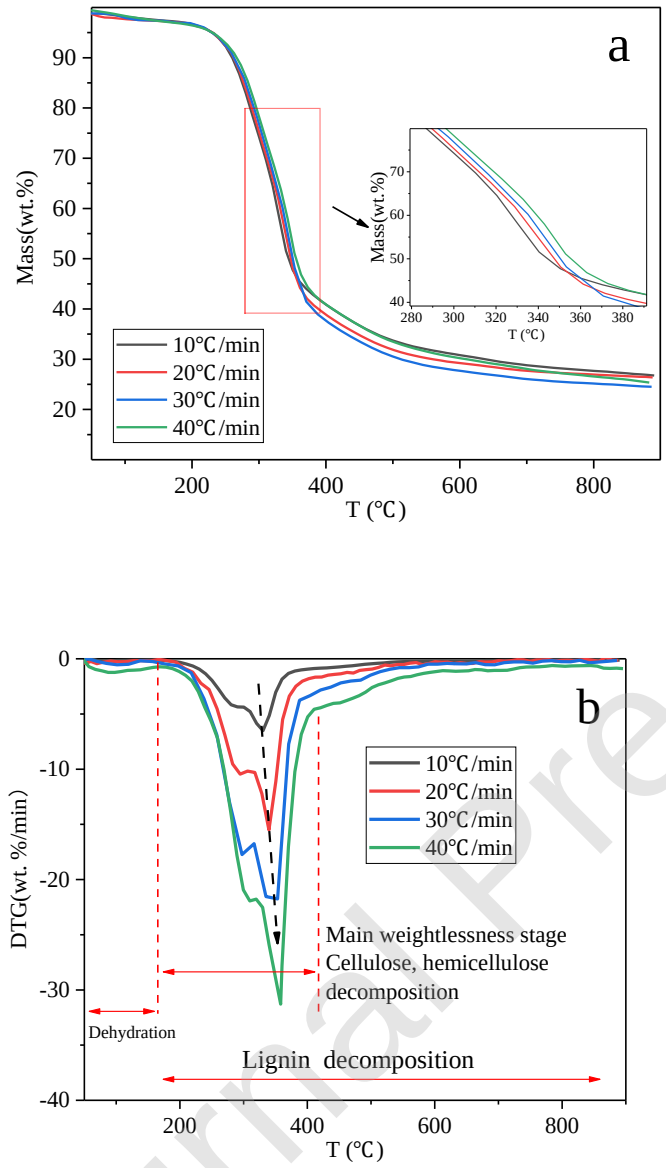

Figure 3 TG (a) and DTG (b) diagrams of corn stover at different heating rates.

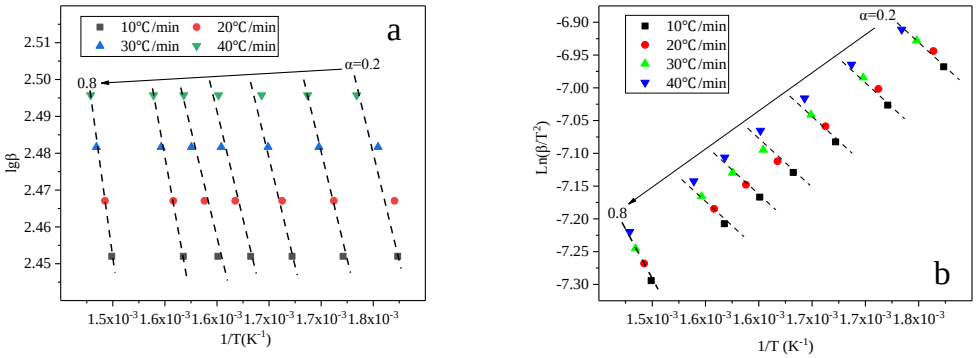

Figure 4 FWO and KAS method for different conversational fraction of corn stover obtained at various heating rates. (a. FWO; b. KAS)

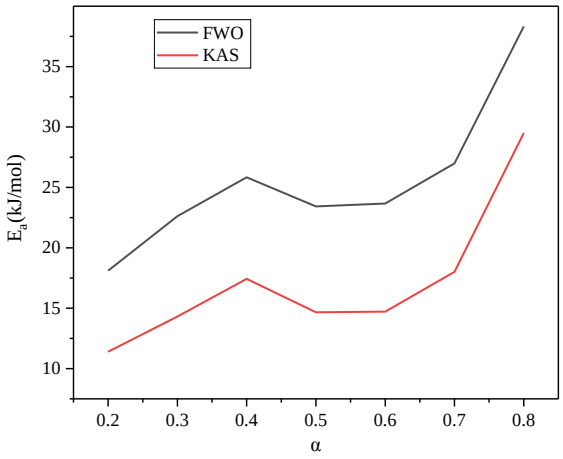

Figure 5 Activation energy of corn stover obtained using the FWO and KAS method.

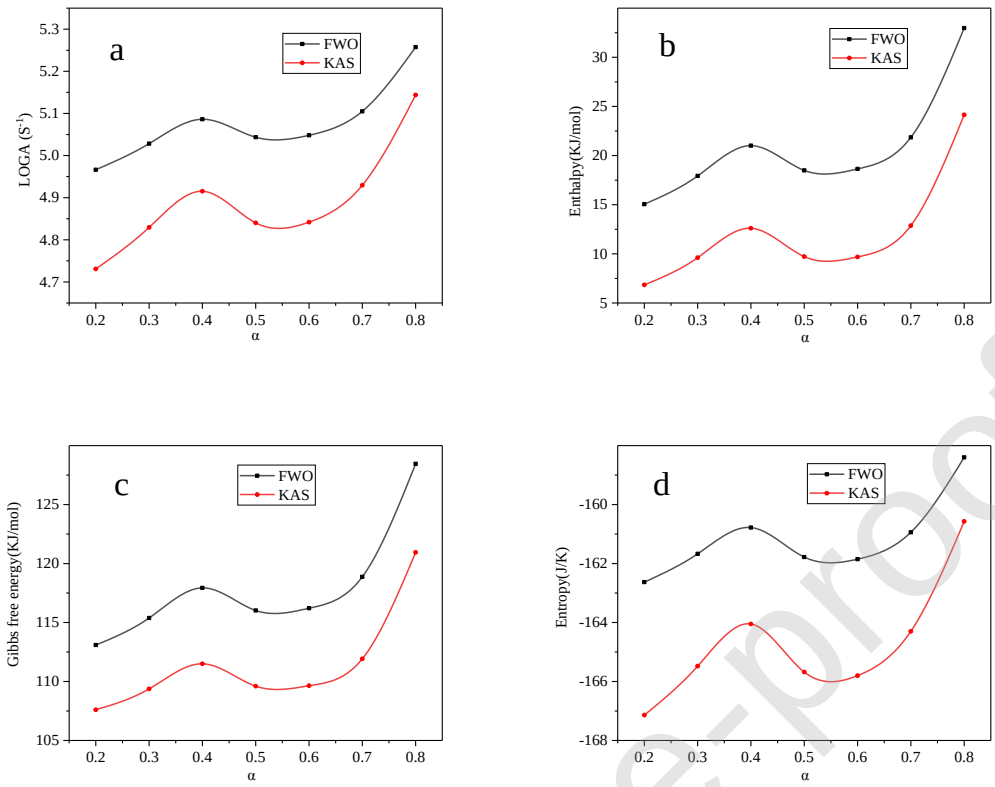

Figure 6 Changes in thermodynamics and kinetics parameters of corn stover using FWO and KAS method at different conversion. a) log 10 (Arrhenius pre-exponential factor) vs conversion, b) Enthalpy

vs conversion c) Gibbs free energy vs conversion d) Entropy vs conversion.

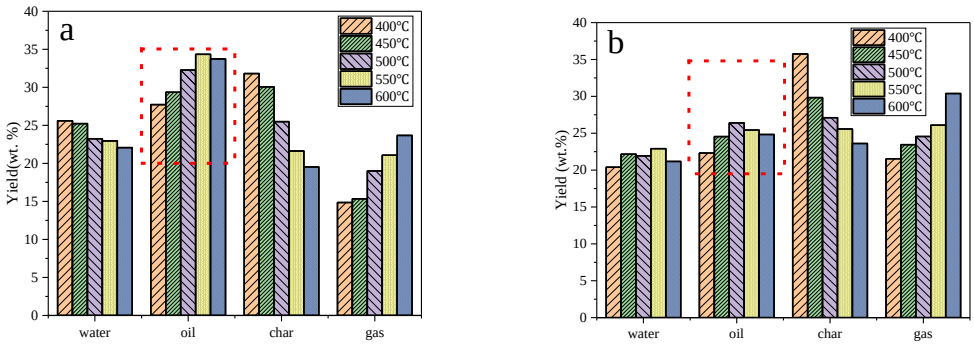

Figure 7 Pyrolysis products distribution of corn stover with varying the temperature (a. infrared heated furnace; b. electrically heated furnace)

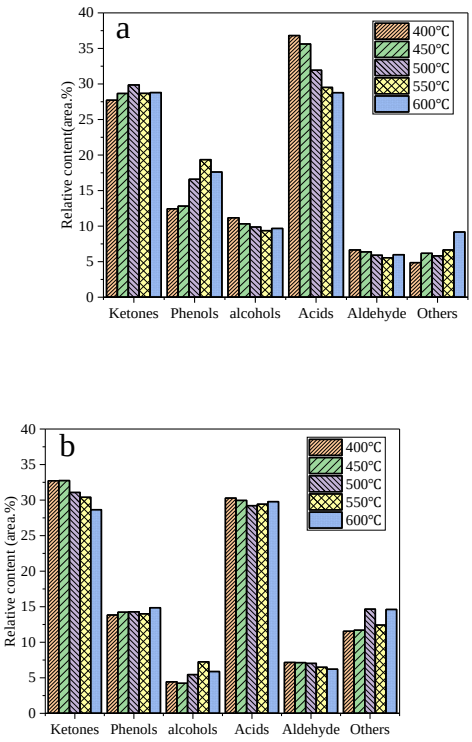

Figure 8 Relative content of main compounds in bio-oil detected by GC-MS analysis (a. infrared heated furnace; b. electrically heated furnace)

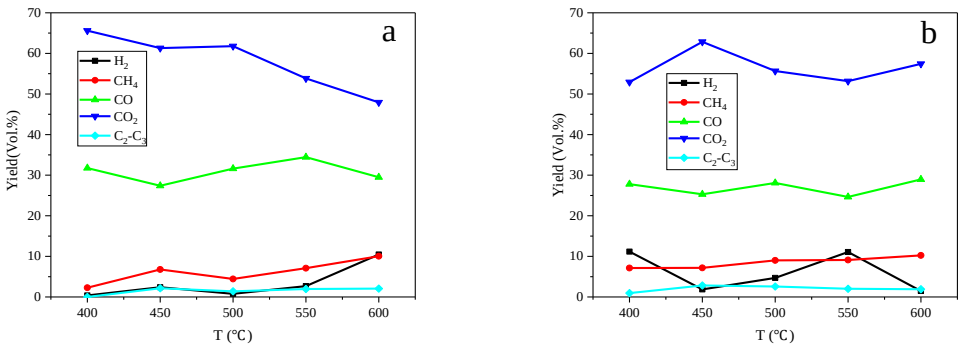

Figure 9 Variation of gas products with increasing temperature. (a. infrared heated furnace; b. electrically heated furnace)

Table 1 Proximate analysis and ultimate analysis of corn stover

Proximate analysis (wt.%)					Ultimate analysis (wt.%, daf)				
Name	M_{ad}	A_{ad}	V_{ad}	FC*	C	H	O*	N	S
Corn stover	10.40	6.70	67.52	15.38	44.87	5.75	48.21	0.97	0.20

*: Calculated by difference; ad: air dried basis; daf: dry ash-free basis.

Table 2 Reaction mechanisms, model names and their f(a) and g(a).

Reaction mechanisms	Symbol	$f(a)$	$g(\alpha)$
Avrami-Erofeev	A3/2	$\frac{3}{2}(1-\alpha)\left[-\ln(1-\alpha)\right]^{\frac{1}{3}}$	$\left[-\ln(1-\alpha)\right]^{\frac{2}{3}}$
Avrami-Erofeev	A2	$2(1-\alpha)\left[-\ln(1-\alpha)\right]^{\frac{1}{2}}$	$\left[-\ln(1-\alpha)\right]^{\frac{1}{2}}$
Avrami-Erofeev	A3	$3(1-\alpha)\left[-\ln(1-\alpha)\right]^{\frac{2}{3}}$	$\left[-\ln(1-\alpha)\right]^{\frac{1}{3}}$
Avrami-Erofeev	A4	$4(1-\alpha)\left[-\ln(1-\alpha)\right]^{\frac{3}{4}}$	$\left[-\ln(1-\alpha)\right]^{\frac{1}{4}}$
One-dimensional diffusion	D1	$\frac{1}{2\alpha}$	α^2
Two-dimensional diffusion	D2	$\left[-\ln(1-\alpha)\right]^{-1}$	$\alpha+(1-\alpha)\ln(1-\alpha)$
Three-dimensional diffusion(Jander)	D3	$\frac{3}{2}(1-\alpha)^{\frac{2}{3}}\left[1-(1-\alpha)^{\frac{1}{3}}\right]^{-1}$	$1-\frac{2}{3\alpha}-(1-\alpha)^{\frac{2}{3}}$
Four-dimensional diffusion (Ginstring-Brounshtein)	D4	$\frac{2}{3}\left[(1-\alpha)^{\frac{1}{3}}-1\right]^{-1}$	$\left[1-(1-\alpha)^{\frac{1}{3}}\right]^2$
Zero-order	F0	1	α
First-order	F1	$1-\alpha$	$-\ln(1-\alpha)$
Second-order	F2	$(1-\alpha)^2$	$(1-\alpha)^{-1}-1$
Third-order	F3	$(1-\alpha)^3$	$\frac{1}{2}\left[(1-\alpha)^{-2}-1\right]$
Power-law	P2	$2\alpha^{\frac{1}{2}}$	$\alpha^{\frac{1}{2}}$
Power-law	P3	$3\alpha^{\frac{2}{3}}$	$\alpha^{\frac{1}{3}}$
Power-law	P4	$4\alpha^{\frac{3}{4}}$	$\alpha^{\frac{1}{4}}$

Contracting cylinder	R2	$2(1-\alpha)^{\frac{1}{2}}$	$1-(1-\alpha)^{\frac{1}{2}}$
Contracting cylinder	R3	$3(1-\alpha)^{\frac{2}{3}}$	$1-(1-\alpha)^{\frac{1}{3}}$

Table 3 DTG curve characteristic parameters and residual mass of corn stover pyrolysis at different heating rates

Heating rate (□/min)	TG		DTG		Residual weight (wt.%)
	T_i (□)	T_f (□)	T_p (□)	R_p (wt. %/min)	
10	269.40	367.70	330.36	-6.50	26.75
20	273.20	378.60	340.20	-15.51	26.36
30	278.00	383.20	353.25	-21.75	24.51
40	287.30	387.90	358.07	-31.29	25.36

T_i: The initial decomposition temperature;

T_f: The terminal decomposition temperature of the most intense stage;

T_p: The peak temperature of DTG;

R_p: The maximum weight loss rate;

Table 4 Kinetic parameters of corn stover sample by using various reaction models at heating rates of 10, 20, 30 and 40 □/min.

Model name	Heating rate(□/min)	E_a（kJ/mol）	R^2
A3/2	10	17.58	0.884
	20	18.29	0.880
	30	20.41	0.892
	40	15.85	0.889
A2	10	17.37	0.948
	20	16.96	0.953
	30	18.16	0.960
	40	15.35	0.917
A3	10	11.58	0.953
	20	11.31	0.961
	30	12.11	0.961
	40	10.23	0.918
A4	10	8.69	0.937
	20	8.48	0.943
	30	9.08	0.920
	40	7.67	0.917
D1	10	15.12	0.994
	20	14.75	0.988
	30	15.76	0.991
	40	13.28	0.984
D2	10	10.91	0.929
	20	10.82	0.928
	30	11.69	0.939
	40	9.64	0.932
D3	10	141.86	0.924
	20	107.66	0.944
	30	102.74	0.938
	40	125.52	0.902
D4	10	9.41	0.974
	20	8.86	0.941
	30	9.26	0.975
	40	8.23	0.923
F0	10	17.40	0.914
	20	16.25	0.926
	30	16.89	0.923
	40	15.20	0.916
F1	10	34.75	0.939
	20	33.92	0.953
	30	36.32	0.960
	40	30.70	0.917
F2	10	79.65	0.914
	20	82.26	0.897
	30	91.41	0.907
	40	71.72	0.847
F3	10	209.46	0.837
	20	231.61	0.833

	30	268.15	0.847
	40	193.45	0.845
P2	10	8.70	0.920
	20	8.13	0.926
	30	8.44	0.919
	40	7.60	0.901
P3	10	5.80	0.912
	20	5.42	0.907
	30	5.63	0.903
	40	5.07	0.914
P4	10	4.35	0.945
	20	4.06	0.908
	30	4.22	0.921
	40	3.80	0.894
R2	10	8.70	0.903
	20	8.13	0.916
	30	8.44	0.919
	40	8.13	0.921
R3	10	5.80	0.932
	20	5.42	0.916
	30	5.63	0.930
	40	5.07	0.908

Table 5 Kinetic parameters calculated by FWO and KAS method

FWO				KAS		
Conversion α	E_a (kJ/mol)	R^2	Average activation energy (kJ/mol)	E_a (kJ/mol)	R^2	Average activation energy (kJ/mol)
0.2	19.61	0.954		11.40	0.981	
0.3	22.62	0.995		14.31	0.988	
0.4	25.84	0.991		17.43	0.981	
0.5	23.43	0.968	25.57	14.66	0.924	17.15
0.6	23.67	0.994		14.72	0.985	
0.7	26.99	0.997		18.01	0.993	
0.8	38.33	0.997		29.51	0.995	

Table 6 Thermodynamic parameters calculated from activation energies of FWO and KAS methods

	FWO				KAS			
α	$A(s^{-1})$	ΔH(kJ/mol)	ΔG(kJ/mol)	ΔS(J/K)	$A(s^{-1})$	ΔH(kJ/mol)	ΔG(kJ/mol)	ΔS(J/K)
0.2	92544.99	15.05	113.09	-162.63	53813.44	6.84	107.60	-167.14
0.3	106744.81	17.92	115.39	-161.67	67512.40	9.61	109.37	-165.48
0.4	121930.14	21.01	117.94	-160.78	82262.11	12.60	111.50	-164.05
0.5	110576.57	18.49	116.02	-161.78	69202.07	9.72	109.60	-165.68
0.6	111722.89	18.64	116.21	-161.85	69481.16	9.69	109.64	-165.80
0.7	127373.53	21.85	118.87	-160.94	85004.33	12.87	111.92	-164.30
0.8	180922.76	32.97	128.46	-158.40	139266.40	24.14	120.94	-160.57